Fizika Nizkikh Temperatur, 2009, v. 35, No. 5, p. 503–509

Linear, diatomic crystal: single-electron states and large-radius excitons

V.M. Adamyan and O.A. Smyrnov

Department of Theoretical Physics, Odessa I.I. Mechnikov National University
2 Dvoryanskaya Str., Odessa 65026, Ukraine
E-mail: smyrnov@onu.edu.ua

Received November 13, 2008, revised January 4, 2009

The large-radius exciton spectrum in a linear crystal with two atoms in the unit cell was obtained using the single-electron eigenfunctions and the band structure, which were found by the zero-range potentials method. The ground-state exciton binding energies for the linear crystal in vacuum appeared to be larger than the corresponding energy gaps for any set of the crystal parameters.

PACS: 73.22.Dj Single particle states;
73.22.Lp Collective excitations;
71.35.Cc Intrinsic properties of excitons; optical absorption spectra.

Keywords: quasione-dimensional semiconductors, zero-range potentials method, single-walled carbon nanotubes, exciton, exciton binding energy.

1. Introduction

The study of the quasione-dimensional semiconductors with the cylindrical symmetry became an urgent problem as soon as investigations of semiconducting nanotubes had been launched. One of the most important trends of research in this field is the study of optical spectra of such systems, which should include the exciton contributions [1–9]. Evidently, the quasione-dimensional large-radius exciton problem can be reduced to the 1D system of two quasi-particles with the potential having Coulomb attraction tail. Due to the parity of the interaction potential the exciton states should split into the odd and even series. In [10] we show that for the bare and screened Coulomb interaction potentials the binding energy of even excitons in the ground state well exceeds the energy gap (in the same work we also discuss the factors, which prevent the collapse of single-electron states in isolated semiconducting single-walled carbon nanotubes (SWCNTs). But the electron-hole (e-h) interaction potential and so the corresponding exciton binding energies may noticeably depend on the electron and hole charge distributions. So it is worth to ascertain whether the effect of seeming instability of single-electron states near the gap is inherent to the all quasione-dimensional semiconductors in vacuum or it maybe takes place only in SWCNTs for the specific localization of electrons (holes) at their surface and weak screening by the bound electrons. That is why we consider here the simplest model of the quasione-dimensional semiconductor with the cylindrical symmetry, namely the linear crystal with two atoms in the unit cell. The electrons (holes) in this crystal are simply localized at its axis.

The aim of this work is only a qualitative analysis of the mentioned effect. For study of electron structure of concerned 1D crystal we apply here the zero-range potentials (ZRPs) method [11,12] (see Sec. 2). The matter is that results on the band structure and single-electron states, obtained by this method for SWCNTs in [13,14], appeared to be in good accordance with the experimental data and results of ab initio calculations related to the band states. For certainty we use the linear crystal parameters (the electron bare mass, lattice parameters) taken from works on nanotubes [13,14]. In Sec. 3 we obtain the e-h bare interaction potential and that screened by the crystal band electrons, and then the large-radius exciton spectrum for the linear crystal in vacuum. All these data are used in Sec. 4, where we present results of calculations for the crystal with different lattice periods (it also means different band structures). As it turns out, the binding energy of even excitons in the ground state well exceeds ($\sim 2-5$ times) the energy gap for the linear crystal in vacuum and the screening by the crystal band electrons is negligible. Note, that this result was obtained within the framework of exactly solvable ZRPs model with feasible parameters. Therefore, the mentioned instability ef-

fect may take place not only for the considered simplest case, but, most likely, also for other quasione-dimensional isolated semiconductors in vacuum.

2. Single-electron band structure and eigenfunctions of band electrons

We have obtained the single-electron states in the linear crystal using the ZRPs method [11,12]. The main point of this method is that the interaction of an electron with atoms or ions of a lattice is described instead of some periodic potential $V(\mathbf{r})$ by the sum of Fermi pseudo-potentials [11]

$$(1/\alpha)\sum_l \delta(\rho_l)(\partial/\partial\rho_l)\rho_l$$

($\rho_l = |\mathbf{r}-\mathbf{r}_l|$, $\mathbf{r}_l$ are the points of atoms location, α is a certain fitting parameter) or equivalently by the set of boundary conditions imposed on the single-electron wave function ψ at points $\mathbf{r}_l$:

$$\lim_{\rho_l\to 0}\left\{\frac{d}{d\rho_l}(\rho_l\psi)(\mathbf{r})+\alpha(\rho_l\psi)(\mathbf{r})\right\}=0\,.$$

The electron wave functions satisfy at that the Schrödinger equation for a free particle for $\mathbf{r}\neq\mathbf{r}_l$. Therefore we seek them for the linear crystal in the form:

$$\psi(\rho_n^A,\rho_n^B)=\sum_{n=-\infty}^{\infty}A_n\frac{\exp(-\kappa\rho_n^A)}{\rho_n^A}+\sum_{n=-\infty}^{\infty}B_n\frac{\exp(-\kappa\rho_n^B)}{\rho_n^B}, \tag{1}$$

where indices A and B denote two monatomic sublattices of the diatomic lattice,

$$\rho_n^A=|\mathbf{r}-\mathbf{r}_n^A| \text{ and } \rho_n^B=|\mathbf{r}-\mathbf{r}_n^B|\,,$$

n numbers all the sublattices points, $\kappa=\sqrt{2m_b|E|}/\hbar$, $E<0$ is the electron energy and m_b is the bare mass. For certainty, following [13,14] we take from now on $m_b\simeq 0.415m_e$ and the ZRP parameter $\alpha=\sqrt{2m_b|E_{\rm ion}|}/\hbar$, where $E_{\rm ion}$ is the ionization energy of an isolated carbon atom. By [13,14], with these α and m_b ZRPs method reproduces single-electron spectra of such quasione-dimensional structures as SWCNTs within an accuracy of existing experiments. One can take infinite limits for the series in (1) even for the finite crystal, because terms of these series decrease exponentially with increasing of n.

According to the ZRPs method the wave functions (1) should satisfy the following boundary conditions at the all sublattices points:

$$\lim_{\rho_l^i\to 0}\left\{\frac{d}{d\rho_l^i}(\rho_l^i\psi)(\mathbf{r})+\alpha(\rho_l^i\psi)(\mathbf{r})\right\}=0\,, \tag{2}$$

here $i=\{A,B\}$ according to each sublattice.

Further we suppose that the linear crystal lies along the z-axis, thus $\mathbf{r}_n^A=nd\mathbf{e}_z$ and $\mathbf{r}_n^B=(nd+a)\mathbf{e}_z$, where $\mathbf{e}_z$ is the z-axis unit vector, a is the distance between atoms in the unit cell of the crystal and $d>2a$ is the distance between the neighbour atoms in each sublattice. Note, that $d=2a$ corresponds to the metallic monatomic crystal and for the case $d<2a$ the smallest distance between atoms in the crystal is $d-a<a$.

Substituting (1) to (2) and applying the Bloch theorem ($A_n=A\exp(iqdn)$, $B_n=B\exp(iqdn)$, q is the electron quasi-momentum) we get two equations for amplitudes A,B:

$$\begin{cases}AQ_1+BQ_2=0\,,\\ AQ_2^*+BQ_1=0\,,\end{cases} \tag{3}$$

where

$$Q_1(\kappa,q)=\alpha-\frac{1}{d}\ln\left(2\left[\cosh\kappa d-\cos qd\right]\right), \tag{4}$$

$$Q_2(\kappa,q)=\sum_{n=-\infty}^{\infty}\frac{\exp(-\kappa|nd+a|+iqnd)}{|nd+a|}. \tag{5}$$

Setting $d=ja$:

$$Q_2(\kappa,q)=$$
$$=\frac{1}{a}\int_0^1\left(\frac{\exp[-\kappa a]}{1-x^j\exp[d(iq-\kappa)]}+\frac{x^{j-2}\exp[\kappa a]}{\exp[d(iq+\kappa)]-x^j}\right)dx \tag{6}$$

for each real $j>2$.

From (3) we get two equations, which define the band structure of the crystal:

$$Q_1(\kappa_1,q)-|Q_2(\kappa_1,q)|=0\,, \tag{7}$$

$$Q_1(\kappa_2,q)+|Q_2(\kappa_2,q)|=0\,. \tag{8}$$

Equation (7) defines the conduction band and equation (8) defines the valence band (see Sec. 4, Fig. 1). So the electron and hole effective masses can be simply obtained from (7) and (8), respectively.

Further, using the Hilbert identity for Green's function of the 3D Helmholtz equation, we obtain the normalized wave functions (1):

$$\psi_{\kappa,q}(\mathbf{r})=\frac{A(\kappa,q)}{\sqrt{L}}\left(\sum_{n=-\infty}^{\infty}\frac{\exp(-\kappa|\mathbf{r}-nd\mathbf{e}_z|+iqnd)}{|\mathbf{r}-nd\mathbf{e}_z|}-\right.$$
$$\left.-\frac{Q_1}{Q_2}\sum_{n=-\infty}^{\infty}\frac{\exp(-\kappa|\mathbf{r}-(nd+a)\mathbf{e}_z|+iqnd)}{|\mathbf{r}-(nd+a)\mathbf{e}_z|}\right), \tag{9}$$

where L is the crystal length and $A(\kappa,q)$ is the normalization factor:

$$A(\kappa, q) = \frac{1}{2}\left(\frac{\kappa d}{\pi} \frac{\cosh \kappa d - \cos qd}{\sinh \kappa d - \Re y} \right)^{1/2},$$

and

$$y = \frac{Q_1}{Q_2} \left(\exp[-iqd] \sinh \kappa a + \sinh \kappa [d-a] \right).$$

3. Exciton spectrum and eigenfunctions. Bare and screened e–h interaction

Using the same arguments as in the 3D case one can show (see, for example [10]), that the wave equation for the Fourier transform ϕ of envelope function in the wave packet from products of the electron and hole Bloch functions, which represents a two-particle state of large-radius rest exciton in a (quasi)one-dimensional semiconductor with period d, is reduced to the following 1D Schrödinger equation:

$$-\frac{\hbar^2}{2\mu}\phi''(z) + V(z)\phi(z) = \mathcal{E}\phi(z), \mathcal{E} = E_{\text{exc}} - E_g, -\infty < z < \infty, \tag{10}$$

where μ is the e–h reduced effective mass and $V(z)$ is the e–h interaction potential:

$$V(z) = -\int_{E_3^d}\int_{E_3^d} \frac{e^2}{((x_1-x_2)^2 + (y_1-y_2)^2 + (z+z_1-z_2)^2)^{1/2}} \times$$
$$\times |u_{c;\kappa,\pi/d}(\mathbf{r}_1)|^2 |u_{v;\kappa,\pi/d}(\mathbf{r}_2)|^2 \, d\mathbf{r}_1 d\mathbf{r}_2, E_3^d = E_2 \times (0 < z < d).$$

Here $u_{c,v;\kappa,q}(\mathbf{r})$ are the Bloch amplitudes of the Bloch wave functions $\psi_{c,v;\kappa,q}(\mathbf{r}) = \exp(iqz) u_{c,v;\kappa,q}(\mathbf{r})$ of the conduction and valence band electrons of the linear crystal, respectively. Using the actual localization of the Bloch amplitudes at the crystal axis, after several Fourier transformations and simplifications we adduce the e-h interaction potential to the following form:

$$V_{r_1,r_2}(z) = -\frac{4e^2 r_1^2}{r_2 d^2} \int_0^\infty \frac{J_1(k) J_1(kr_2/r_1)}{k^4} \times$$
$$\times \left(\frac{k}{r_1}(|d-z| + |d+z| - 2|z|) + \exp\left[-\frac{k}{r_1}|d-z| \right] + \right.$$
$$\left. + \exp\left[-\frac{k}{r_1}|d+z| \right] - 2\exp\left[-\frac{k}{r_1}|z| \right] \right) dk, \tag{11}$$

where J is the Bessel function of the first kind and r_1 (r_2) is the radius of the electron (hole) wave functions transverse localization

$$r_{1,2} = \left(2\int_{E_2} r_{2D}^2 \int_0^L |u_{c,v;\kappa,q}(z, \mathbf{r}_{2D})|^2 \, dz \, d\mathbf{r}_{2D} \right)^{1/2},$$

where $\mathbf{r}_{2D}$ is the transverse component of the radius-vector, $q = \pi/d$ and $\kappa = \kappa_{1,2}(\pi/d)$ correspond to the conduction and valence bands edges at the energy gap (according to (7) and (8), respectively). Equation (10) with the potential given by (11) defines the spectrum of large-radius exciton in the linear, diatomic crystal if the screening effect by the crystal electrons is ignored. Actually, the screening of the potential (11) by the band electrons is insignificant.

Indeed, following the Lindhard method (so-called RPA), to obtain the e–h interaction potential $\varphi(\mathbf{r})$, screened by the electrons of linear lattice, let us consider the Poisson equation:

$$-\Delta\varphi(\mathbf{r}) = 4\pi(\rho^{\text{ext}}(\mathbf{r}) + \rho^{\text{ind}}(\mathbf{r})) \tag{12}$$

where $\mathbf{r}$ is the radius-vector, $\rho^{\text{ext}}(\mathbf{r})$ is the density of extraneous charge and $\rho^{\text{ind}}(\mathbf{r})$ is the charge density induced by the extraneous charge.

By (12) the screened e–h interaction potential may be written as:

$$\varphi(\mathbf{r}) = 4\pi \int_{E_3} (\rho^{\text{ext}}(\mathbf{r}') + \rho^{\text{ind}}(\mathbf{r}')) G(\mathbf{r}, \mathbf{r}') \, d\mathbf{r}', \tag{13}$$

where $G(\mathbf{r}, \mathbf{r}') = 1/(4\pi|\mathbf{r} - \mathbf{r}'|)$ is Green's function of the 3D Poisson equation.

Let $E^0(q)$ and $\psi^0_{\kappa,q}(\mathbf{r}) = \exp(iqz) u^0_{\kappa,q}(\mathbf{r})$ be the band energies and corresponding Bloch wave functions of the crystal electrons and $E(q)$, $\psi_{\kappa,q}(\mathbf{r})$ be those in the presence of the extraneous charge. Then

$$\rho^{\text{ind}}(\mathbf{r}) = -e\sum_q [f(E(q))|\psi_{\kappa,q}(\mathbf{r})|^2 - f(E^0(q))|\psi^0_{\kappa,q}(\mathbf{r})|^2], \tag{14}$$

where f is the Fermi–Dirac function. Using the transverse localization of the Bloch wave functions near the crystal axis, we get in the linear in φ approximation:

$$\rho^{\text{ind}}(z', \mathbf{r}'_{2D}) = -e^2 \sum_{q,q'} \frac{1}{E_{g;q,q'}} \int_0^L \int_{E_2} u_{v;\kappa_2,q'}(z, \mathbf{r}_{2D}) \times$$
$$\times u^*_{c;\kappa_1,q}(z, \mathbf{r}_{2D}) d\mathbf{r}_{2D} \, \varphi(z) \exp[iz(q'-q)] dz \times$$
$$\times u^*_{v;\kappa_2,q'}(z', \mathbf{r}'_{2D}) u_{c;\kappa_1,q}(z', \mathbf{r}'_{2D}) \exp[iz'(q-q')], \tag{15}$$

where $E_{g;q,q'} = E_c(q) - E_v(q')$. Here and further $\varphi(z)$ is the e–h interaction potential averaged in E_2 over the region of the Bloch wave functions transverse localization and over the lattice period d along the crystal axis.

Due to the periodicity of the Bloch amplitudes ρ^{ind} may be written as:

$$\rho^{\text{ind}}(\mathbf{r}') = -\frac{e^2 N}{L}\sum_{q,q'}\frac{C(q,q';d)}{E_{g;q,q'}}\varphi(q-q')\times$$
$$\times\, u^*_{v;\kappa_2,q'}(\mathbf{r}')u_{c;\kappa_1,q}(\mathbf{r}')\exp[iz'(q-q')], \qquad (16)$$

where

$$C(q,q';d) = \int_0^d\int_{E_2} u^*_{c;\kappa_1,q}(z,\mathbf{r}_{2D})u_{v;\kappa_2,q'}(z,\mathbf{r}_{2D})d\mathbf{r}_{2D}dz$$

and N is the number of unit cells in the crystal.

Further, after several transformations we obtain from (13) and (16) the one-dimensional Fourier transform of the potential φ:

$$\varphi(k) = \frac{\varphi_0(k)}{\varepsilon(k)},$$
$$\varepsilon(k) = 1+\frac{e^2N^2}{2\pi^2}\int_{-\pi/d}^{\pi/d}\frac{|C(q,q-k;d)|^2}{E_{g;q,q-k}}dq\widetilde{K}_0(k)\frac{2\sin(kd/2)}{kd} \qquad (17)$$

where φ_0 is the Fourier transform of the averaged electrostatic potential induced by ρ^{ext} and $\widetilde{K}_0(k)$ is the modified Bessel function of the second kind averaged over $\mathbf{r}_{2D}$ and $\mathbf{r}'_{2D}$ in the region of the Bloch wave functions transverse localization in E_2, namely

$$\widetilde{K}_0(k) = \frac{1}{(\pi r_1 r_2)^2}\int_{E_2^{r_1}}\int_{E_2^{r_2}} K_0(|k||\mathbf{r}_{2D}-\mathbf{r}'_{2D}|)d\mathbf{r}_{2D}d\mathbf{r}'_{2D},$$

$$E_2^{r_i} = (0\le r_{2D}\le r_i)\times(0\le\beta\le 2\pi).$$

In the long-wave limit we get:

$$|C(q,q-k;d)|^2_{k\to 0}\approx|U(q;d)|^2\,k^2,$$
$$U(q;d) = \int_0^d\int_{E_2} u^*_{c;\kappa_1,q}(z,\mathbf{r}_{2D})\frac{\partial}{\partial q}u_{v;\kappa_2,q}(z,\mathbf{r}_{2D})\,d\mathbf{r}_{2D}dz. \qquad (18)$$

Using of the Schrödinger equation for the orthogonal Bloch wave functions $\psi_{\kappa,q}(\mathbf{r})$ yields

$$U(q;d) =$$
$$= \frac{i\hbar^2}{E_{g;q,q}m_b}\int_0^d\int_{E_2}\psi^*_{c;\kappa_1,q}(z,\mathbf{r}_{2D})\frac{\partial}{\partial z}\psi_{v;\kappa_2,q}(z,\mathbf{r}_{2D})d\mathbf{r}_{2D}dz. \qquad (19)$$

Hence, in the long-wave limit the screened quasione-dimensional electrostatic potential induced by a charge e_0, distributed with the density:

$$\rho^{\text{ext}}(z,\mathbf{r}_{2D}) = \frac{e_0}{\pi R^2 d}(\Theta[z+d/2]-\Theta[z-d/2])\times$$
$$\times(\Theta[r_{2D}]-\Theta[r_{2D}-R]),\ R>0,$$
$$\Theta[x-x_0] = \begin{cases}0, x<x_0,\\ 1, x>x_0,\end{cases}$$

in accordance with (17) and (19), is given by the expression

$$\varphi(z) = \frac{8e_0r_1}{\pi d^2}\int_0^\infty\frac{(1/k^2)\sin^2(kd/2r_1)\widetilde{K}_0(k/r_1)\cos(kz/r_1)}{1+g_d(kr_1/d)\sin(kd/2r_1)\widetilde{K}_0(k/r_1)}dk \qquad (20)$$

with

$$g_d = \left(\frac{e\hbar^2}{\pi r_1 m_b}\right)^2\int_{-\pi/d}^{\pi/d}\frac{1}{E^3_{g;q,q}}\left|\left\langle\psi_{c;\kappa_1,q}\left|\frac{\partial}{\partial z}\right|\psi_{v;\kappa_2,q}\right\rangle\right|^2 dq. \qquad (21)$$

According to equation (9) the dimensionless screening parameter g_d may be also written as:

$$g_d = \left(\frac{16e}{\hbar d r_1}\right)^2 m_b\int_0^{\pi/d}\frac{A_c^2(\kappa_1,q)A_v^2(\kappa_2,q)}{(\kappa_2^2(q)-\kappa_1^2(q))^5}\times$$
$$\times\left|\left(1+\frac{Q_1(\kappa_1,q)Q_1(\kappa_2,q)}{Q_2^*(\kappa_1,q)Q_2(\kappa_2,q)}\right)\int_{\kappa_1}^{\kappa_2}Q_1(\kappa,q)\,d\kappa-\frac{Q_1(\kappa_1,q)}{Q_2^*(\kappa_1,q)}\times\right.$$
$$\left.\times\int_{\kappa_1}^{\kappa_2}Q_2^*(\kappa,q)\,d\kappa-\frac{Q_1(\kappa_2,q)}{Q_2(\kappa_2,q)}\int_{\kappa_1}^{\kappa_2}Q_2(\kappa,q)\,d\kappa\right|^2 dq. \qquad (22)$$

Note, that κ_1 and κ_2 are the implicit functions of q defined by (7) and (8), respectively.

It appears, that g_d calculated according to (22) for d varying in the interval $[2.1a,3a]$ are about 10^{-6}.

4. Discussion. Stabilization of single-electron states

Using Eqs. (7) and (8) we obtained the band structure (see Fig. 1) and the electrons and holes effective masses for the linear crystal of dimers for different values of the ratio $j = d/a$ of its period d and the distance a between atoms in dimers. Besides, using wave equation (10) and potentials (11) and (20) we found the large-radius exciton energy spectrum in the crystal for the bare e–h interaction and e–h interaction screened by the bound electrons of the crystal. We present here results for the crystal with $j\in[2.1,3]$. Contrary to the single-band metallic crystal with $j=2$, the crystals with $j>2$ are semiconductors with band gaps varying from zero to the difference between the electron levels in an isolated dimer. Particularly, the crys-

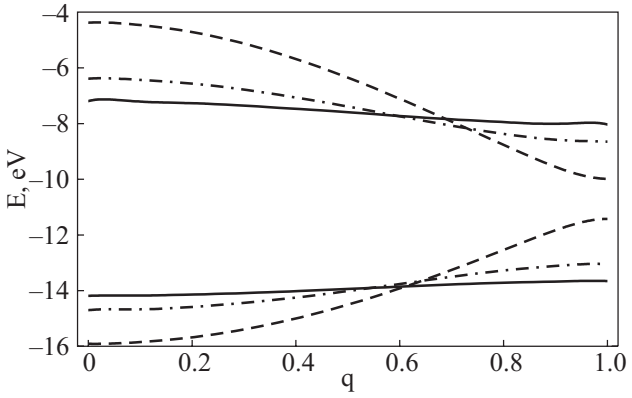

Fig. 1. The band structure of the linear crystal with parameters: $j = 2.1$ (dashed line), $j = 2.5$ (dot-dashed line) and $j = 3$ (solid line); q in units of π / d. The upper and lower bands correspond to equation (7) and (8), respectively.

tals with $j = 2.001$ and realistic values of a and α (as in nanotubes and some 1D polymer chains) are narrow-gap semiconductors, in which excitons may possess binding energies about ~ 10 meV, but the crystals with $j = 2.1$ are already wide-gap (~ 1 eV) semiconductors with strongly bound e–h pairs, and the crystals with $j = 3$ are almost flat band semiconductors, but their electrons and holes at the energy gaps ($q = \pi / d$) still have the finite effective masses (these electrons and holes form the excitons in the crystals). For certainty, the distance a we have chosen equal to the graphite in-plane parameter 0.142 nm. The ZRP interaction parameter $\alpha = 11.01\ \text{nm}^{-1}$ corresponds to the ionization energy of an isolated carbon atom ($E_{\text{ion}} = 11.255$ eV).

As one can see from table 1 the obtained from (22) dimensionless screening parameter $g_d << 1$ for the all considered values of j. So, it turns out that the screening of the e–h interaction potential by the band electrons in the linear, diatomic crystal may be ignored. This result could be expected since the considered model of linear crystal is close to that of the electron gas confined to a cylindrical well. In the latter case, for which the separation of the angular variables takes place, the states with different quantum numbers m of the angular momentum play the role of electron bands. Accordingly, the matrix element $|\langle \psi_c | \partial / \partial z | \psi_v \rangle|$ from (21) for the direct transitions between bands with different m appears to be identically equal to zero. This is why only the binding energies of excitons with unscreened interaction potential are listed in table 1.

To obtain estimates of the main linear crystal characteristics we considered several limiting cases. In the case of $d >> a$ (or $j >> 1$) and $a = \text{const}$ equations (7) and (8) can be reduced to $\alpha - \kappa_{1,2} \mp \exp[-\kappa_{1,2} a] / a = 0$, thus bands become flat ($\kappa_{1,2}$ do not depend on q) and the band gap tends to the finite value $(\hbar^2 / 2m_b)(\kappa_2^2 - \kappa_1^2)$ (for $a = = 0.142$ nm it is about 6.3 eV), hence the reduced effective mass and exciton binding energy tend to infinity, while the exciton radius $r_{\text{exc}} \sim \hbar^2 / \mu e^2$ tends to zero. Therefore, the large-radius exciton theory is actually appropriate ($r_{\text{exc}} >> a$) for excitons in the linear, diatomic crystal only when its period d runs the interval $(2a, 2.4a)$ (e.g., r_{exc} is $\sim 9a$ for $j = 2.1$ and $\sim 2a$ for $j = 2.4$). If $d = \text{const}$, but $a \to 0$, the conduction band moves to the region of positive energies and at some critical value of a disappears, while the valence band shifts correspondingly to the region of deep negative energies.

Table 1 shows that the ground-state exciton binding energies for the linear, diatomic crystals with any value of the ratio j are greater than the corresponding energy gaps. Note, that according to the same calculations, but with the bare mass $m_b = m_e$, the ground-state exciton binding energy for the linear crystal in vacuum appears significantly greater than the energy gap. We should note also, that the ground-state binding energies of excitons in the linear crystal with different periods d in vacuum, calculated using the 1D analogue of the Ohno potential [15] instead of potential (11), remain greater than the corresponding energy gaps. Particularly, for $d = 2.3a$ calculations with the 1D unscreened Ohno potential with the energy parameter U taken from [16] ($U = 11.3$ eV) and [17] ($U = 16$ eV) give the ground-state exciton binding energies $\mathcal{E}_{0;\text{even}} = 5.90$ eV and $\mathcal{E}_{0;\text{even}} = 7.63$ eV, respectively, while $E_g = 3.31$ eV (see table 1). Thus, all calculations

Table 1. Band gaps E_g and reduced effective masses μ according to (7), (8); radii of the electrons and holes transverse localization r_1 and r_2, respectively; screening parameter g_d according to (22) and the exciton binding energies $\mathcal{E}$ of the even and odd series for the linear, diatomic crystal according to equation (10) with potential (11) for different values of the ratio $j = d / a$.

j	E_g, eV	μ (m_e)	r_1, nm	r_2, nm	g_d (10^{-6})	$\mathcal{E}_{0;\text{even}}$, eV	$\mathcal{E}_{1;\text{odd}}$, eV	$\mathcal{E}_{0;\text{even}} / E_g$
2.1	1.4422	0.041	0.070	0.0611	0.7235	–6.90	–0.5939	4.7845
2.3	3.3146	0.125	0.080	0.0569	2.4716	–8.9992	–2.0631	2.715
2.5	4.403	0.2199	0.088	0.0549	2.7036	–9.5352	–3.4812	2.1656
3	5.6281	0.5665	0.0994	0.0551	1.1206	–9.6588	–5.8421	1.7162

made on the base of solvable zero-range potentials model indicate the instability of the single-electron states in the vicinity of the energy gap with respect to the formation of excitons. This might be a shortage of this model, but it is worth mentioning that results obtained on one-particle states in real 1D systems, like SWCNTs [13,14], within its framework agree with existing experimental data in limits of accuracy of the latter.

The stability of single-electron states of 1D semiconductors with respect to the exciton formation in vacuum can be explained by bringing multi-particle contributions into the picture. With the advent of some number of excitons in the quasione-dimensional crystal the additional screening appears, which is caused by a rather great polarizability of excitons in the longitudinal electric field. This collective contribution of born excitons into the crystal permittivity returns the lowest exciton binding energy $\mathcal{E}_{0;\text{even}}$ into the energy gap and so blocks further spontaneous transitions to the exciton states. To show this let us consider the model of linear crystal immersed into the gas of excitons with dielectric constant ε_{exc} confined to the region of linear crystal carriers transverse localization, namely: cylinder with radius r_1 and axis coinciding with that of linear crystal (from now on, for estimates, we assume that electron and hole have the same transverse localization radius). In this case it is easy to show that the e–h interaction potential is given by:

$$\varphi(z) = \frac{16e^2 r_1}{\pi d^2}\int_0^\infty \frac{\sin^2(kd/2r_1)\cos(kz/r_1)}{\varepsilon_{\text{exc}} k^4}\times$$
$$\times\left(1-\frac{2K_1(k)I_1(k)}{k(\varepsilon_{\text{exc}}K_0(k)I_1(k)+K_1(k)I_0(k))}\right)dk\,, \quad (23)$$

where I_i and K_i are the modified Bessel functions of the order i of the first and second kind, respectively. Further, like in [18], we use the known elementary relation between the permittivity of exciton gas and its polarizability α in the direction of linear crystal

$$\varepsilon_{\text{exc}} = 1+4\pi\alpha,\ \alpha = 2e^2 n\sum_k \frac{|\langle\Psi_0|\mathbf{r}|\Psi_k\rangle|^2}{\mathcal{E}_0-\mathcal{E}_k}\,,$$

where n is the bulk concentration of excitons, Ψ_0 and $\mathcal{E}_0$ are the exciton eigenfunction and binding energy, which correspond to the ground state, and Ψ_k and $\mathcal{E}_k$ are those, which correspond to the all excited states of exciton. Thus, the upper and lower limits for α are:

$$\frac{2e^2 n}{\mathcal{E}_0-\mathcal{E}_1}|\langle\Psi_0|\mathbf{r}|\Psi_1\rangle|^2 \le \alpha \le \frac{2e^2 n}{\mathcal{E}_0-\mathcal{E}_1}\sum_k|\langle\Psi_0|\mathbf{r}|\Psi_k\rangle|^2 =$$
$$= \frac{2e^2 n}{\mathcal{E}_0-\mathcal{E}_1}|\langle\Psi_0|\mathbf{r}^2|\Psi_0\rangle|\,,$$

where Ψ_1 and $\mathcal{E}_1$ correspond to the lowest excited exciton state. Hence, one can obtain the upper and lower limits for n:

$$\frac{\varepsilon_{\text{exc}}-1}{4\pi}\frac{\mathcal{E}_{0;\text{even}}-\mathcal{E}_{1;\text{odd}}}{2e^2}\left|\int_{-\infty}^{\infty} z^2|\phi_0(z)|^2\,dz\right|^{-1} \le n\,,$$
$$n \le \frac{\varepsilon_{\text{exc}}-1}{4\pi}\frac{\mathcal{E}_{0;\text{even}}-\mathcal{E}_{1;\text{odd}}}{2e^2}\left|\int_{-\infty}^{\infty} z\phi_0(z)\phi_1(z)\,dz\right|^{-2}\,, \quad (24)$$

where each ϕ is the component of Fourier transform of the corresponding exciton envelope function, it depends only on the distance z between the electron and hole. At that, ϕ_0 is the even solution of (10) with potential (23), which corresponds to the exciton ground state and satisfies the boundary condition $\phi'(0)=0$, and ϕ_1 is the odd solution of the same equation, which corresponds to the lowest excited exciton state and satisfies the boundary condition $\phi(0)=0$.

Varying ε_{exc} in (23) substituted into the wave equation (10) one can match $\mathcal{E}_{0;\text{even}}$ to the forbidden band width. Further, $\mathcal{E}_{1;\text{odd}}$ can be obtained from the same equation with the fixed ε_{exc} and with the corresponding boundary condition. All these magnitudes allow to calculate from (24) the rough upper and lower limits for the critical concentration of born excitons n_c, which is sufficient to return $\mathcal{E}_{0;\text{even}}$ into the energy gap. Further, knowing n_c we can calculate the shift of the forbidden band edges, which move apart due to the transformation of some single-electron states into excitons. This results in the enhancement of energy gap

$$\delta E_g \simeq \frac{(\pi\hbar\tilde{n}_c)^2}{2\mu} \quad (25)$$

like in [19] and [20]. Here $\tilde{n}_c = n_c\pi r_1^2$ is the linear critical concentration of excitons, and r_1 is the radius of electron wave functions transverse localization at the linear crystal axis.

In accordance with (24) the described model yields $\tilde{n}_c \sim 180\ \mu\text{m}^{-1}$ ($\sim 3\%$ of the atoms number in the crystal) and $\sim 400\ \mu\text{m}^{-1}$ ($\sim 7\%$) for the linear crystal with $j = 2.1$ and $j = 2.3$, respectively, while by (25) the corresponding δE_g are ~ 300 meV and ~ 500 meV in the same order. Here, however, we should mention that for SWCNTs both the measured in [19,20] and estimated in the same manner [18] values of $\delta E_g / E_g$ appeared to be two–four times less.

Note, finally, that the instability of the single-electron states weakens or disappears for linear crystals immersed into dielectric media. As it was shown in [9] by the example of the poly-para-phenylenevinylene 1D chain or in [16,17,21] by the example of SWCNTs the environmental effect may substantially decrease the excitons binding energies. Indeed, for the linear crystal in media even with

permittivity about $\varepsilon \sim 2$–3 (e.g., like in [16] or [17]) the ground-state exciton binding energy becomes smaller than the energy gap.

This work was supported by the Ministry of Education and Science of Ukraine, Grant#0106U001673.

1. M.J. O'Connell, S.M. Bachilo, C.B. Huffman, V.C. Moore, M.S. Strano, E.H. Haroz, K.L. Rialon, P.J. Boul, W.H. Noon, C. Kittrell, J. Ma, R.H. Hauge, R.B. Weisman, and R.E. Smalley, *Science* **297**, 593 (2002).
2. S.M. Bachilo, M.S. Strano, C. Kittrell, R.H. Hauge, R.E. Smalley, and R.B. Weisman, *Science* **298**, 2361 (2002).
3. M. Ichida, S. Mizuno, Y. Saito, H. Kataura, Y. Achiba, and A. Nakamura, *Phys. Rev.* **B65**, 241407(R) (2002).
4. F. Wang, G. Dukovic, L.E. Brus, and T.F. Heinz, *Science* **308**, 838 (2005).
5. E. Chang, G. Bussi, A. Ruini, and E. Molinari, *Phys. Rev. Lett.* **92**, 196401 (2004).
6. T. Ando, *J. Phys. Soc. Jpn.* **66**, 1066 (1997).
7. A. Jorio, G. Dresselhaus, and M.S. Dresselhaus (eds.), *Carbon Nanotubes. Advanced Topics in the Synthesis, Structure, Properties and Applications*, Springer-Verlag, Berlin, Heidelberg (2008).
8. S. Abe, *J. Photopolym. Sci. Technol.* **6**, 247 (1993).
9. A. Ruini, M.J. Caldas, G. Bussi, and E. Molinari, *Phys. Rev. Lett.* **88**, 206403 (2002).
10. V.M. Adamyan and O.A. Smyrnov, *J. Phys. A: Math. Theor.* **40**, 10519 (2007).
11. S. Albeverio, F. Gesztesy, R. Høegh-Krohn, and H. Holden, *Solvable Models in Quantum Mechanics. Texts and Monographs in Physics*, Springer, New York (1988).
12. Yu.N. Demkov and V.N. Ostrovskii, *Zero-Range Potentials and Their Applications in Atomic Physics*, Plenum, New York (1988).
13. S.V. Tishchenko, *Fiz. Nizk. Temp.* **32**, 1256 (2006) [*Low Temp. Phys.* **32**, 953 (2006)].
14. V. Adamyan and S. Tishchenko, *J. Phys.: Condens. Matter* **19**, 186206 (2007).
15. K. Ohno, *Theor. Chim. Acta* **2**, 219 (1964).
16. J. Jiang, R. Saito, Ge.G. Samsonidze, A. Jorio, S.G. Chou, G. Dresselhaus, and M.S. Dresselhaus, *Phys. Rev.* **B75**, 035407 (2007).
17. R.B. Capaz, C.D. Spataru, S. Ismail-Beigi, and S.G. Louie, *Phys. Rev.* **B74**, 121401(R) (2006).
18. V.M. Adamyan, O.A. Smyrnov, and S.V. Tishchenko, *J. Phys.: Conf. Series* **129**, 012012 (2008).
19. Y. Ohno, S. Iwasaki, Y. Murakami, S. Kishimoto, S. Maruyama, and T. Mizutani, *Phys. Rev.* **B73**, 235427 (2006).
20. O. Kiowski, S. Lebedkin, F. Hennrich, S. Malik, H. Rösner, K. Arnold, C. Sürgers, and M.M. Kappes, *Phys. Rev.* **B75**, 075421 (2007).
21. V. Perebeinos, J. Tersoff, and P. Avouris, *Phys. Rev. Lett.* **92**, 257402 (2004).